Supporting information:

Figure and Table captions:

Figures:

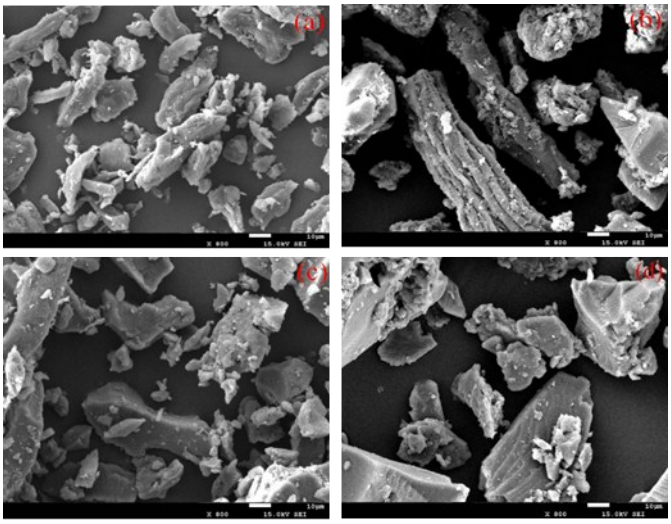

Fig. S1 SEM images of XG (a), XG-Cl (b), XG-NH_2 (c) and XG-NH_2 loaded by Cu^{2+} (d)

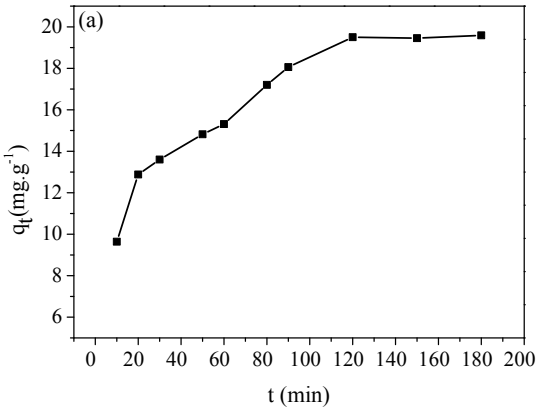
(a)
20
18
16
14
12
10
8
6
q_t(mg.g^{-1})
0
20
40
60
80
100
120
140
160
180
200
t (min)

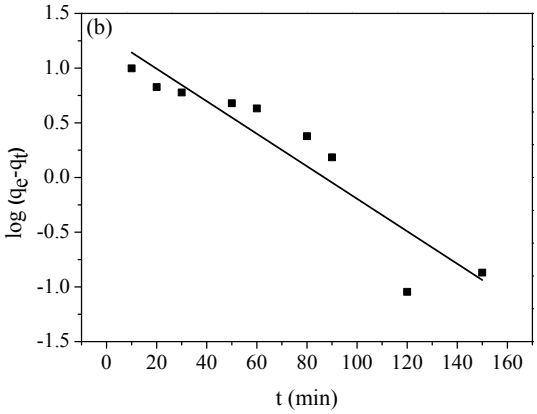
(b)
1.5
1.0
0.5
0.0
-0.5
-1.0
-1.5
log (q_e-q_t)
0
20
40
60
80
100
120
140
160
t (min)

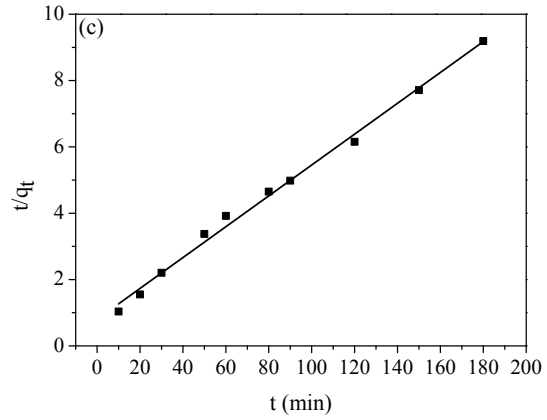

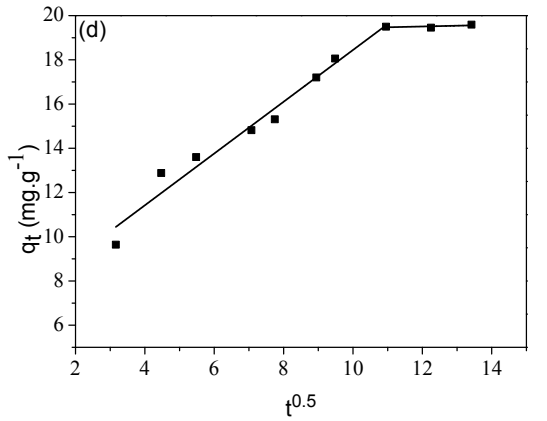

Fig. S2 Effect of contact time on the removal of Cu^{2+} (a), the pseudo-first-order kinetic model (b), the pseudo-second-order kinetic model (c), and intra-particle diffusion plots (d) for Cu^{2+} adsorption by XG-NH_2.

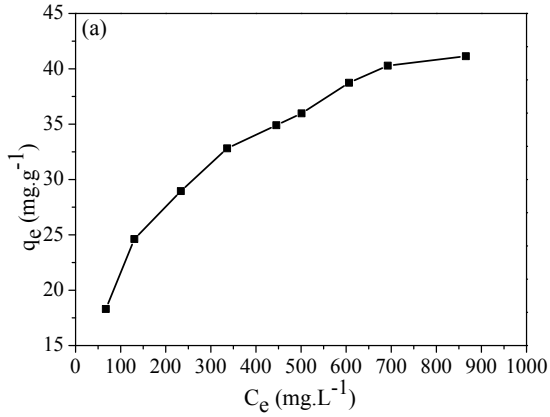

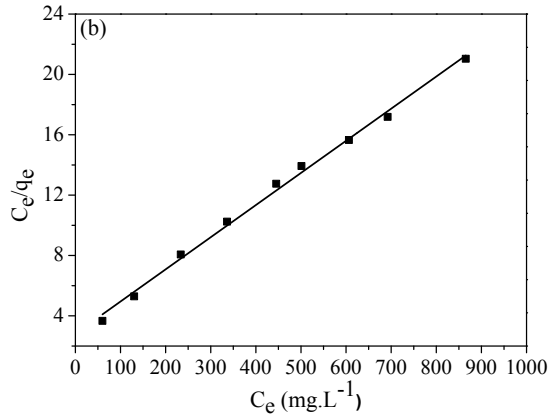

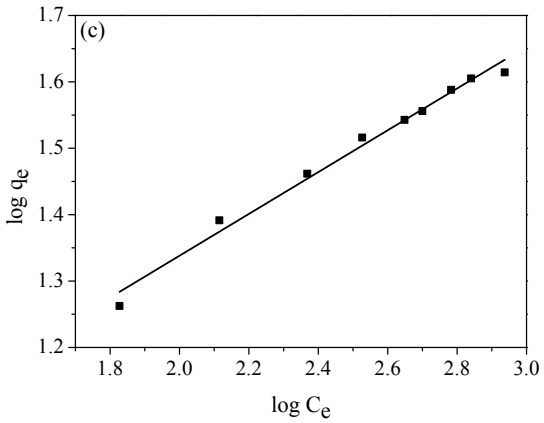

Fig. S3 Adsorption isotherm of Cu^{2+} adsorption (a), Langmuir (b) and Freundlich (c) adsorption isotherm for Cu^{2+} adsorption by XG-NH_2

Tables:

Table S1 The parameters of different kinetic model

pseudo-first order	pseudo-second order	Intra-particle diffusion
$q_{e,\exp} = 19.59 mg.g^{-1}$		
$q_{e,cal} = 19.57 mg.g^{-1}$	$q_{e,cal} = 21.50 mg.g^{-1}$	
R^2=0.855	R^2=0.994	R^2=0.967
$k_1 = 0.03422\ \min^{-1}$	$k_2 = 0.002163 g.mg^{-1}.\min^{-1}$	$kp = 1.170 mg.h^{0.5}.g^{-1}$

Table S2 Langmuir and Freundlich isotherm parameters

Langmuir adsorption isotherm	Freundlich adsorption isotherm

$q_{max}(mg.g^{-1})$	$b(L.mg^{-1})$	R^2	R_L	n	$K_f(mg.g^{-1})$	R^2
46.95	132.4	0.996	0-1	3.176	5.107	0.986

Table S3 The adsorption capacity of different divalent cations by XG-NH_2

Divalent cation	Cu^{2+}	Pb^{2+}	Cd^{2+}	Ni^{2+}	Zn^{2+}	Co^{2+}	Ca^{2+}
Adsorption capacity (mg. g^{-1})	20.22	11.07	9.192	6.393	4.030	2.472	1.883